V. PHYSICAL ELECTRONICS AND SURFACE PHYSICS*

Academic and Research Staff

Prof. R. E. Stickney

Graduate Students

V. S. Aramati
A. E. Dabiri
C-N. Lu
D. V. Tendulkar

A. EXPERIMENTAL MEASUREMENTS OF THE SPEED DISTRIBUTION OF D_2 DESORBED FROM A NICKEL SURFACE

1. Introduction

This study is a continuation of a previous experimental investigation of the spatial distributions of hydrogenic molecules (H_2, D_2, HD) desorbed from a polycrystalline nickel surface.[1] We report data on the speed distribution of D_2 desorbed from a polycrystalline nickel surface.

2. Experimental Apparatus and Procedures

The principal features of the experimental apparatus have been described previously.[2] In the present case, the speed distribution can be measured only in the direction normal to the Ni surface. Molecules are supplied to the Ni surface by permeation as described previously.[1]

3. Experimental Results

In Fig. V-1 the time-of-flight curve for D_2 desorbed from polycrystalline Ni at 1073°K is shown. The filled circles were computed for the case of an equilibrium gas having a temperature equal to that of the Ni sample.[2] The amplitude of the computed curve has been normalized to fit the maximum of the experimental curve, but no steps were taken to force the maxima to occur at the same point on the time scale. The agreement is sufficiently close to suggest that the actual speed distribution corresponds to that of a gas in complete thermal equilibrium at the temperature of the Ni surface. Similar data were obtained at different temperatures for D_2 and no significant deviations from the equilibrium case were observed.

*This work was supported principally by the National Aeronautics and Space Administration (Grant NGR 22-009-091), and in part by the Joint Services Electronics Programs (U.S. Army, U.S. Navy, and U.S. Air Force) under Contract DA 28-043-AMC-02536(E).

To prove that the time-of-flight curve shown in Fig. V-1 is a direct consequence of D_2 desorbed from the Ni surface rather than from D_2 and other species in the background gas of the beam chamber, we repeated the measurement after reducing D_2 pressure

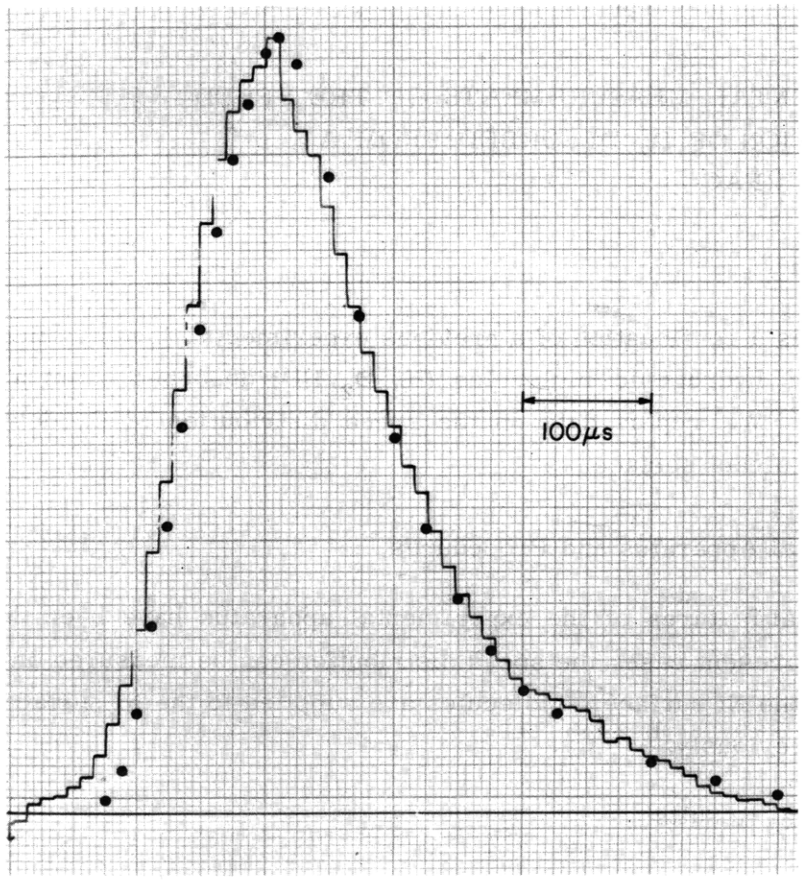

Fig. V-1. Time-of-flight data for D_2 desorbed from a polycrystalline Ni surface at 1073°K. The filled circles were computed for the case of an equilibrium gas having a temperature equal to that of the Ni sample (ref. 2, p. 22, Eq. (1)).

behind the Ni membrane to the degree that the permeation rate was negligible at 1073°K. To simulate the conditions of the preceding test, we maintained the Ni membrane at 1073°K and leaked D_2 into the beam chamber at a rate sufficient to bring the background pressure up to the same level. In this case the detector signal was so weak that the time-of-flight curve was of the order of the noise level. We conclude that the form of the time-of-flight curve in Fig. V-1 is not distorted significantly by the background gas or other side effects.

4. Discussion of Results

a. Comparison with Existing Experimental Results

No comparisons are possible in the case of our speed distribution data because we are not aware of any previous measurements of this type for hydrogenic molecules desorbed from solid surface. (Through personal communication with van Willigen, we have learned that he has recently measured the mean speed of H_2 desorbed from a polycrystalline Ni surface.) The only existing data that we have found on the speed distributions of desorbed particles are for the desorption of K from a variety of solids.[3]

5. Comparison with Existing Theoretical Models

We know of only two theoretical models that provide predications of the spatial and speed distributions of desorbed molecules. The first is the equilibrium model, whose development has been summarized by Loeb,[4] and it predicts a diffuse ($\cos^1 \theta$) spatial distribution and an equilibrium (Maxwellian) speed distribution. The second is the model developed by van Willigen[5] from the activated-adsorption model of Lennard-Jones.[6] We shall derive expressions for the spatial and speed distributions predicted on the basis of this activated-adsorption model.

a. Spatial Distribution

According to the activated-adsorption model shown in Fig. V-2, the gas-solid interaction potential may be of such a nature that the atomic and molecular states of adsorption are separated by an activation-energy barrier of height E_a. For simplicity, we shall assume that E_a is constant over the entire surface. Although it is expected that E_a is a periodic function related to the positions of the atoms of the solid surface, the variation in amplitude may be quite small because the molecule-solid potential involves more than nearest-neighbor interactions.

From kinetic theory, the rate at which molecules collide with a solid surface of unit area is, for equilibrium conditions,[7]

$$Z = p(2\pi mkT)^{-1/2} \tag{1}$$

where p, m, and T are the pressure, molecular mass, and temperature of the gas. A more detailed description of the collision rate is obtained by considering only those molecules having speeds between v and v + dv, and directions within the solid angle $d\omega = \sin\theta\, d\theta d\phi$, where θ and ϕ are defined with respect to the solid lattice in Fig. V-3. The differential collision rate for this portion of the impinging molecules is[7]

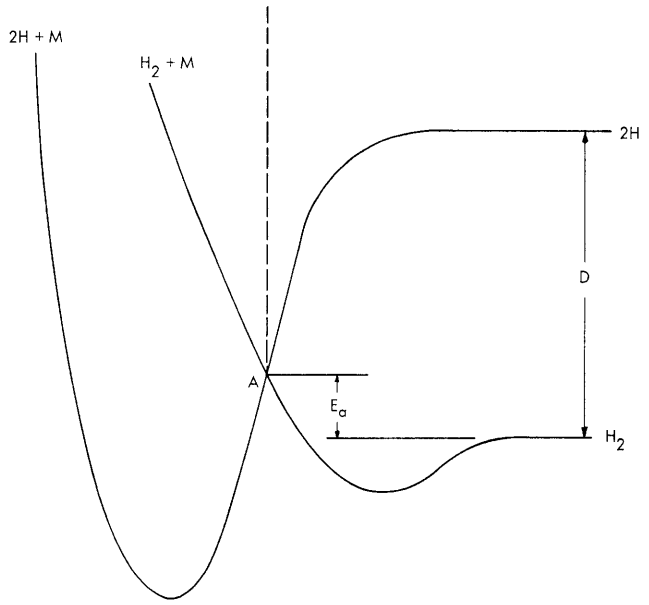

Fig. V-2. Schematic representation of the gas-solid interaction potentials for the case of activated dissociative adsorption of H_2 on the surface of solid M. E_a is the activation energy separating the molecular (H_2 + M) and atomic (2H + M) adsorption states, and D is the dissociation energy of H_2.

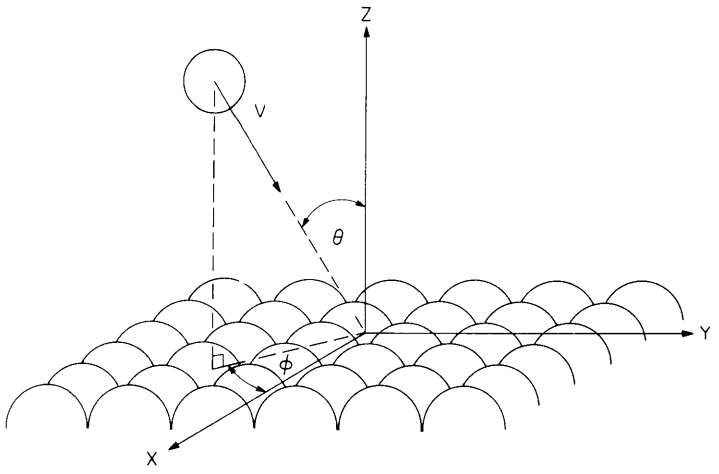

Fig. V-3. Geometry of gas-solid interaction. The quantities v, θ, and ϕ refer to a state sufficiently far from the surface that the gas-solid interaction forces are negligible.

$$d^3Z = \frac{n}{\pi^{3}/2}\left(\frac{v}{a}\right)^3 \exp\left[-\left(\frac{v}{a}\right)^2\right] \sin\theta \cos\theta \, d\theta d\phi dv \tag{2a}$$

$$= \frac{2Z}{\pi a}\left(\frac{v}{a}\right)^3 \exp\left[-\left(\frac{v}{a}\right)^2\right] \sin\theta \cos\theta \, d\theta d\phi dv, \tag{2b}$$

where n is the number density, and $a = (2kT/m)^{1/2}$. From the definitions above it follows that

$$\int_{v=0}^{\infty}\int_{\phi=0}^{2\pi}\int_{\theta=0}^{\pi/2} d^3Z = Z. \tag{3}$$

The equilibration probability, ζ, is defined as the fraction of the collisions that result in adsorption. The differential equilibration probability, $d^3\zeta$, is

$$d^3\zeta = \frac{d^3\Gamma}{d^3Z}, \tag{4}$$

where $d^3\Gamma$ is the differential adsorption rate (that is, the rate at which molecules of class (v, θ, ϕ) are equilibrated). It is assumed that the definition given in Eq. 4 represents an average over all of the impact points and energy states of the solid that are available to molecules in the class (v, θ, ϕ), as well as an average over all orientations and internal states (vibration and rotation) of the impinging molecules.

Integration of Eq. 4 over all possible values of v gives

$$d^2\zeta = \frac{d^2\Gamma}{d^2Z} = \frac{d^2\Gamma}{Z \cos\theta \, d\omega/\pi} \tag{5}$$

and integration of this over ϕ and θ gives the total equilibration probability,

$$\zeta = \frac{\Gamma}{Z}. \tag{6}$$

Molecules impinging with speed v at angle θ and ϕ will be able to adsorb dissociatively $\left[\frac{1}{2} A_2(g) \rightleftharpoons A(ad)\right]$ only if their energies are large enough to carry them over barrier E_a. That is, the differential equilibration probability of molecules in class (v, θ, ϕ) is

$$d^3\zeta = \begin{cases} 0 & \text{if } 1/2m\,(v\cos\theta)^2 < E_a \\ \zeta_o & \text{if } 1/2m\,(v\cos\theta)^2 \geq E_a \end{cases} \tag{7}$$

where ζ_o is a transmission coefficient representing the fact that some molecules with sufficient energy will not pass over E_a because of quantum-mechanical reflection. We

shall simplify the following discussion by assuming that ζ_o is independent of v, θ, and ϕ. If the gas phase is in equilibrium with the solid, then from Eq. 5 we obtain

$$d^2\zeta = \frac{d^2\Gamma}{d^2Z} = \frac{1}{d^2Z}\int_0^\infty d^3\zeta d^3Z \tag{8}$$

which, with the aid of Eq. 7, may be expressed as

$$d^2\zeta = \int_{v^*}^\infty 2\zeta_o\left(\frac{v}{a}\right)^3 \exp\left[-\left(\frac{v}{a}\right)^2\right] dv/a \tag{9a}$$

$$= \zeta_o\left[1 + \frac{E_a}{kT}\sec^2\theta\right]\exp\left(-\frac{E_a}{kT}\sec^2\theta\right), \tag{9b}$$

where the lower limit of integration is $v^* = \left(\frac{2E_a}{m}\right)^{1/2}\sec\theta$, which follows from Eq. 7. Therefore the ratio of $d^2\zeta$ for angle of incidence θ to that for normal incidence (θ=0) is

$$\frac{d^2\zeta(\theta)}{d^2\zeta(0)} = \frac{E_a + kT\cos^2\theta}{(E_a+kT)\cos^2\theta}\exp\left(-\frac{E_a}{kT}\tan^2\theta\right) \tag{10}$$

and, with the aid of Eq. 5, the corresponding ratio of the differential adsorption rates is

$$\frac{d^2\Gamma(\theta)}{d^2\Gamma(0)} = \frac{d^2\zeta(\theta)}{d^2\zeta(0)}\cos\theta = \frac{E_a + kT\cos^2\theta}{(E_a+kT)\cos\theta}\exp\left(-\frac{E_a}{kT}\tan^2\theta\right). \tag{11}$$

It is important to notice that this equation is the angular distribution of only those molecules in the gas phase that can pass over the barrier. This distribution changes as the molecules enter the force field of the surface and, at the point of A (Fig. V-2) where the molecular potential energy curve intercepts the atomic potential energy curve, they have a new distribution which we call $X(\theta)$.

Now, we would like to use the detailed balance principle to predict the angular distribution of molecules in the gas phase desorbed from the solid surface. The use of the detailed balance is valid only for those cases in which the equilibrated particles can be distinguished from the nonequilibrated particles. For example, if a model enables one to define a boundary in phase space that effectively separates the states of equilibrated adsorbed particles from those of free particles, then this boundary may be used to distinguish equilibrated particles from nonequilibrated particles. In the case of the activated adsorption model, we shall assume that the vertical line drawn from the top of the adsorption barrier (point A in Fig. V-2) is a boundary at which the only molecules

crossing in the outgoing direction are those equilibrated to the solid. Therefore, the detailed balance principle can be applied at this point and what it says is that the differential rate of adsorption must be balanced at equilibrium by an equal but opposite differential rate of desorption from the adsorbate phase. Consequently, according to this principle, the spatial distribution of desorbed molecules at point A is equal to the spatial distribution of adsorbed molecules at this point which we defined as $X(\theta)$. This distribution changes as the molecules escape from the force field of surface and they attain a distribution corresponding to Eq. 11 when they reach the gas phase because between the gas phase and the barrier only a reversible mechanical process is involved according to this simple activated adsorption model. Therefore, the predicted spatial distribution of the desorbed molecules is of the form of Eq. 11 which is identical to that used by van Willigen[5] to explain his experimental observation that the angular distribution of hydrogen desorbing from various metals is not simply proportional to cos θ. Figure V-4

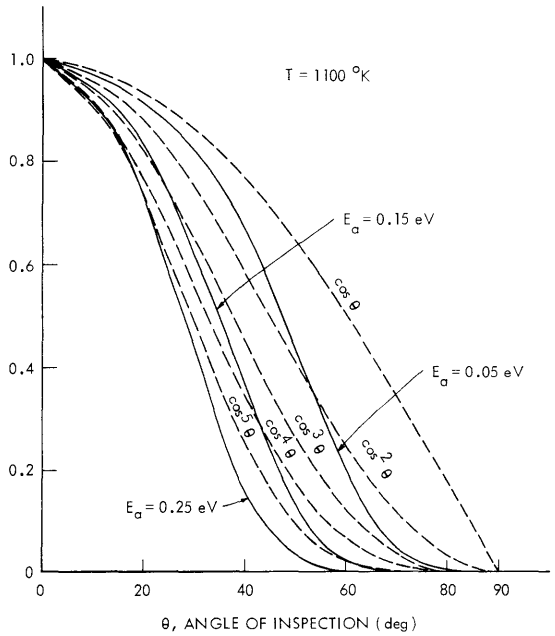

Fig. V-4.

Spatial distributions of desorbed molecules according to the activated adsorption model.

shows this distribution for three different values of the activation energy, E_a, at T = 1100°K. Since our experimental data[1] can be described approximately by $\cos^d \theta$ with $d \approx 4.5$, we estimate from Fig. V-4 that the corresponding value of E_a is between 0.15 and 0.25 eV.

b. Speed Distribution

We shall begin by determining the speed distribution of only those molecules in the gas phase that can be adsorbed on the surface, and then by using the detailed balance principle, we shall come up with the speed distribution of desorbed molecules. We treat

this problem only in the direction normal to the surface because we are measuring the molecular desorption speed distribution only in the normal direction.

The differential collision rate per unit solid angle of molecules impinging in the normal direction, according to Eq. 2b, is

$$dZ = \frac{2Z}{\pi a}\left(\frac{v}{a}\right)^3 \exp\left[-\left(\frac{v}{a}\right)^2\right] dv. \tag{12}$$

The differential equilibration probability, $d\zeta$, is

$$d\zeta = \frac{d\Gamma}{dZ}, \tag{13}$$

where $d\Gamma$ is the differential adsorption rate (that is, the rate at which molecules of class v are equilibrated). Molecules impinging with speed v will be able to adsorb dissociatively only if their energy is large enough to carry them over barrier E_a. That is,

$$d\zeta = \begin{cases} 0 & \text{if } \frac{1}{2}mv^2 < E_a \\ \zeta_o & \text{if } \frac{1}{2}mv^2 \geq E_a \end{cases} \tag{14}$$

Substituting this equation in Eq. 13, we get

$$d\Gamma = \begin{cases} 0 & \text{if } v < v^* \quad (15a) \\ \frac{2\zeta_o Z}{\pi a}\left(\frac{v}{a}\right)^3 \exp\left[-\left(\frac{v}{a}\right)^2\right] dv & \text{if } v > v^* \quad (15b) \end{cases}$$

where

$$v^* = \left(\frac{2E_a}{m}\right)^{1/2}.$$

It is important to notice that Eq. 15b represents the differential adsorption rate of only those molecules in the gas phase that are normal to the surface and have sufficient energy that they can pass over the barrier. The speed distribution of these molecules changes as the molecules enter the force field of the surface, and at point A they have a new distribution that we call Y(v). Now we follow the same argument that we employed in the spatial distribution case and, by the principle of detailed balance, the differential desorption rate of molecules at point A is equal to the differential adsorption rate of molecules at this point which we defined as Y(v). This distribution changes as the molecules escape from the force field of surface, and they attain a distribution corresponding to Eq. 15 when they reach the gas phase, because between the gas phase and

the barrier only a reversible mechanical process is involved according to this simple activated-adsorption model.

Now we have to transform this distribution to the time-of-flight coordinate in order to be able to compare it with the experimental measurements. For $v > v^*$, Eq. 15b is identical to the corresponding expression for an equilibrium gas, and we may use the results derived in Appendix A. Therefore, for the limiting case of zero chopping time, we obtain from Eq. A. 12 the following expression for the instantaneous number density of desorbed molecules in the detector

$$n(\bar{t}_i) = \frac{1.85}{\bar{t}_i^4} e^{-\frac{1}{\bar{t}_i^2}}, \qquad \text{(A. 12)}$$

where $\bar{t}_i$ is the dimensionless flight time defined by

$$\bar{t}_i = \frac{t\alpha}{L}.$$

Here, t is the time measured from the instant the chopper opens, L is the distance from the chopper to the detector, and $\alpha = (2kT/m)^{1/2}$. Since there are no desorbed molecules having $v < v^*$, Eq. A.12 is zero throughout the range $\frac{\alpha}{v^*} < \bar{t}_i < \infty$ (that is, no molecules reach the detector after time $t = L/v^*$, which corresponds to $\bar{t}_i = \frac{\alpha}{v^*}$). The resulting time-of-flight curves, $n(\bar{t}_i)$, are shown in Fig. V-5 for two values of $\bar{t}^o$, where

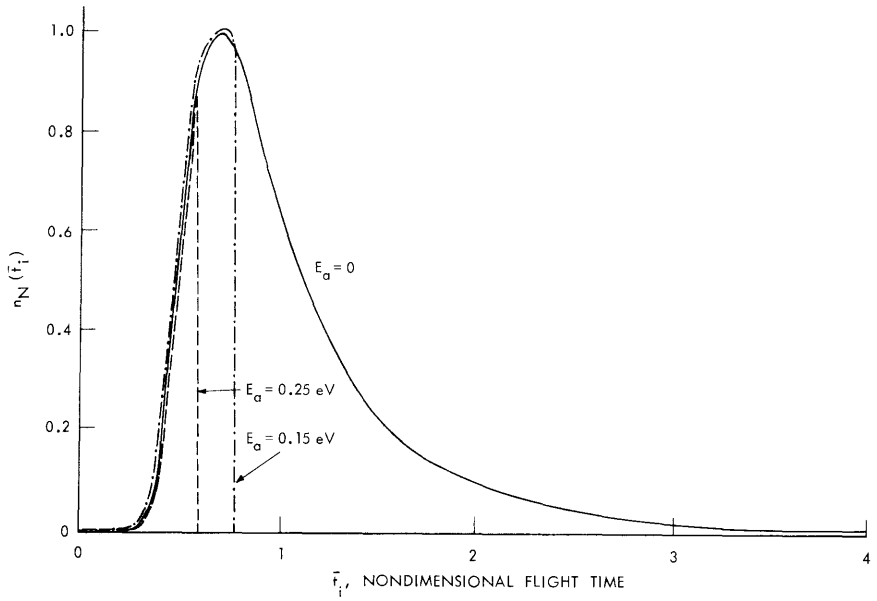

Fig. V-5. Time-of-flight curve for zero chopping time according to the activated adsorption model.

$$\bar{t}^{o} \equiv \frac{a}{v^{*}} = (kT/E_a)^{1/2}. \tag{16}$$

The values of $\bar{t}^{o}$ were chosen to correspond to E_a equal to 0.15 and 0.25 eV, the upper and lower bounds inferred from our spatial distribution data, and to T = 1073°K, the temperature of the Ni membrane in our time-of-flight measurements.

In the case of finite chopping time, the cutoff will not be a vertical line because the amplitude of the time-of-flight distribution at time t no longer corresponds to molecules having speeds that differ only infinitesimally from v = L/t. In order to obtain the shape of this cutoff, we use Eq. A. 8,

$$n(t_i) = \frac{2L^3}{a^4} \int_0^{t^*} \Gamma(t_c) \frac{e^{-\frac{L^2}{a^2(t_i-t_c)^2}}}{(t_i-t_c)^4} dt_c, \tag{A. 8}$$

where $t^* = t_i$ for $t_i < t_{co}$ and $t^* = t_{co}$ for $t_i > t_{co}$, and t_i is the time of arrival at the detector of molecules that passed through the chopper at time t_c, where $0 \leq t_c \leq t_{co}$, with t_{co} being the total time that the chopper is open. The magnitude of $n(t_i)$ corresponds to the contributions of molecules having all possible values of t_c but arriving at the detector at time t_i. These molecules do not have the same speed, and their speeds vary from a minimum at $t_c = 0$ to a maximum at $t_c = t_{co}$. Since the present model predicts that the minimum speed is v^*, we conclude that molecules passing through the chopper at time t_c cannot contribute to $n(t_i)$ if t_c is less than a critical value, t_c^*, defined by the relation

$$t_i - t_c^* = \frac{L}{v^*} \tag{17}$$

or

$$t_c^* = t_i - \frac{L}{v^*} = t_i - t^o,$$

where $t^o \equiv L/v^*$. Therefore the new distribution will be

$$n_N(t_i) = \frac{2L^3\Gamma}{a^4} \int_{t^{**}}^{t^*} \frac{e^{-\frac{L^2}{a^2(t_i-t_c)^2}}}{(t_i-t_c)^4} dt_c, \tag{18}$$

where $t^{**} = 0$ for $t_c^* < 0$ and $t^{**} = t_i - t^o$ for $t_c^* \geq 0$. Notice that this distribution begins to differ from Eq. A. 8 at $t_i = \frac{L}{v^*}$, and it goes to zero at $t_i = \frac{L}{v^*} + t_{co}$. Integration of Eq. 18 leads to the following equation expressed in

dimensionless form:

$$\bar{n}_N(\bar{t}_i) = \frac{1}{\bar{t}_{co}} \left\{ \frac{1}{\bar{t}^o} e^{-\frac{1}{\bar{t}^{o2}}} - \frac{1}{\bar{t}_i - \bar{t}^*} e^{-\frac{1}{(\bar{t}_i - \bar{t}^*)^2}} + \frac{\sqrt{\pi}}{2} \left[\operatorname{erf}\left(\frac{1}{\bar{t}_i - \bar{t}^*}\right) - \operatorname{erf}\left(\frac{1}{\bar{t}^o}\right) \right] \right\}$$

where

$$\bar{t}^o = \frac{t^o a}{L}.$$

This distribution is plotted in Fig. V-6 for D_2 at 1073°K and E_a equal to 0, 0.15, and 0.25 eV. As mentioned previously, our spatial distribution measurements indicate that E_a is between 0.15 and 0.25 eV if the activated adsorption model is approximately valid.

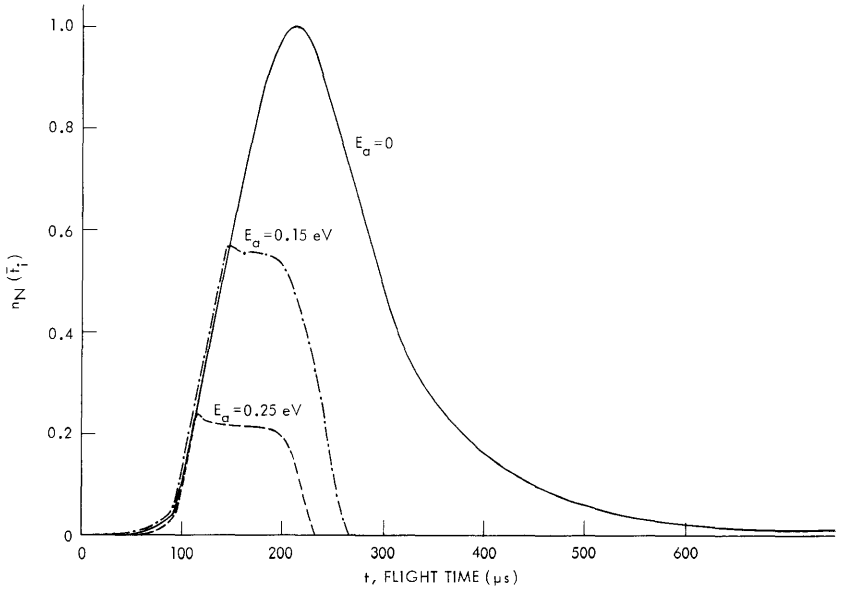

Fig. V-6.
Time-of-flight curve for finite chopping time according to the activated adsorption model.

Therefore, we would expect the time-of-flight distribution to fall between the two curves shown in Fig. V-6, whereas our measurements (Fig. V-1) are observed to agree closely with the distribution for an equilibrium gas (i.e., the curve for $E_a = 0$ in Fig. V-6). Because of this discrepancy, we conclude that the activated adsorption model is not valid.

APPENDIX A

Effect of Finite Chopping Time on Time-of-Flight Distribution

In the time-of-flight technique (TOF) for measurement of the speed distribution, a small segment of the beam is chopped mechanically at a known distance from the

detector. Part of this pulse then passes through the ionization detector. The molecules ionized in the ionization region go through the detection system, and the TOF curve is recorded. The object of this Appendix is to consider the effect of finite chopping time on the TOF curve. Similar analyses have been reported by Scott.[8]

To start, we have to transform the speed distribution function from speed to time coordinates. The Maxwellian speed distribution function is[9]

$$f(v)\,dv = 4\pi^{-1/2}\, n v^2/a^3\, e^{-v^2/a^2}\, dv \tag{A. 1}$$

where $a \equiv (2kT/m)^{1/2}$. Assuming free molecular flow, the distribution of the rate of molecules that arrive at the detector within a solid angle $d\omega$ with speeds between v and v + dv is

$$\Gamma(v)\,dv = v\, f(v)\, dv d\omega. \tag{A. 2}$$

The total rate is

$$\Gamma = \int_0^\infty v\, f(v)\, dv d\omega = \frac{2na\, d\omega}{\pi^{1/2}}. \tag{A. 3}$$

Substituting Eq. A. 3 into Eq. A. 2 for $d\omega$ gives

$$\Gamma(v)\,dv = 2\Gamma\, v^3/a^4\, e^{-v^2/a^2}\, dv. \tag{A. 4}$$

To transform this function to the time coordinate we use the relation $t = \frac{L}{v}$, where L is the distance from chopper to ionizer. The result is

$$g(t)\,dt = -2\Gamma\, L^4/a^4\, e^{-\frac{L^2}{a^2t^2}}\, \frac{dt}{t^5}. \tag{A. 5}$$

This function is the distribution of the rate at which molecules arrive at the detector within the time t to t + dt. (Zero time is defined as the instant that the chopper opens.) This function is correct if t_{co}, the time that the chopper is open, is negligible. In practice, there is always a finite t_{co} for which the distribution should be corrected. t_c is defined as the time that the shutter has been open. Now, the rate at which molecules arrive at the detector, $\Gamma(t_c)$, is a function of t_c, and Eq. A. 5 should be integrated over the time that the shutter is open. Before integration, we should note that t in Eq. A.5 has to be changed to $t_i - t_c$, where t_i is the time that molecules, which start at time t_c at the chopper plane, arrive at the detector. Therefore Eq. A. 5 can be written as

$$h(t_c, t_i)\, dt_c dt_i = 2\Gamma(t_c)\, \frac{L^4}{a^4}\, \frac{e^{-\frac{L^2}{a^2(t_i-t_c)^2}}}{(t_i-t_c)^5}\, dt_c dt_i \qquad \text{(A. 6)}$$

where $h(t_c, t_i)$ is rate of arrival of molecules that start from the chopping plane at t_c and reach the detector at t_i.

We should note that $dt = -dt_c$, but not $dt = dt_i - dt_c$ because we would like to find the contributions of all molecules having t_c from zero to t_{co} at a fixed value of t_i. To find this contribution, we integrate Eq. A. 6 to obtain

$$1(t_i)\, dt_i = \frac{2L^4\, dt_i}{a^4} \int_0^{t^*} \Gamma(t_c)\, \frac{e^{-\frac{L^2}{a^2(t_i-t_c)^2}}}{(t_i-t_c)^5}\, dt_c, \qquad \text{(A. 7)}$$

where $t^* = t_i$ for $t_i < t_{co}$ and $t^* = t_{co}$ for $t_i > t_{co}$, and where $1(t_i)$ is the rate of arrival of molecules at the detector at time t_i. The density at the detector due to this arrival rate is obtained by dividing Eq. A. 7 by the molecular speed, $L/(t_i-t_c)$:

$$n(t_i) = \frac{2L^3}{a^4} \int_0^{t^*} \Gamma(t_c)\, \frac{e^{-\frac{L^2}{a^2(t_i-t_c)^2}}}{(t_i-t_c)^4}\, dt_c. \qquad \text{(A. 8)}$$

Assuming the shutter function to be rectangular, Eq. A. 8 may be integrated to obtain

$$n(t_i) = \frac{\Gamma}{a}\left\{\frac{L}{at_i}\, e^{-\left(\frac{L}{at_i}\right)^2} - \frac{L}{a\left(t_i-t^*\right)}\, e^{-\frac{L}{a^2\left(t_i-t^*\right)^2}} + \frac{\sqrt{\pi}}{2}\left[\operatorname{erf}\left(\frac{L}{a\left(t_i-t^*\right)}\right) - \operatorname{erf}\left(\frac{L}{at_i}\right)\right]\right\}. \qquad \text{(A. 9)}$$

To write this equation in dimensionless form, we define $\bar{t} = \frac{ta}{L}$ and $\bar{n} = \frac{nL}{t_{co}}$, and obtain

$$\bar{n}(\bar{t}_i) = \frac{1}{\bar{t}_{co}}\left\{\frac{1}{\bar{t}_i}\, e^{-\frac{1}{\bar{t}_i^2}} - \frac{1}{\bar{t}_i - \bar{t}^*}\, e^{-\frac{1}{\left(\bar{t}_i-\bar{t}^*\right)^2}} + \frac{\sqrt{\pi}}{2}\left[\operatorname{erf}\left(\frac{1}{\bar{t}_i - \bar{t}^*}\right) - \operatorname{erf}\left(\frac{1}{\bar{t}_i}\right)\right]\right\}. \qquad \text{(A. 10)}$$

In the limiting case of $t_{co} \to 0$, it can be shown that Eq. A.10 reduces to

$$\bar{n}(\bar{t}_i) = \frac{2}{\bar{t}_i^4} e^{-\frac{1}{\bar{t}_i^2}}. \tag{A.11}$$

This distribution is maximum at $\bar{t}_i = \frac{\sqrt{2}}{2}$ where $\bar{n} = 1.08$. Therefore, by normalizing Eq. A.11 with respect to this maximum, we obtain

$$\bar{n}_{No}(\bar{t}_i) = \frac{1.85}{\bar{t}_i^4} e^{-\frac{1}{\bar{t}_i^2}} \tag{A.12}$$

A. E. Dabiri, R. E. Stickney

References

1. A. E. Dabiri and R. E. Stickney, Quarterly Progress Report No. 97, Research Laboratory of Electronics, M. I. T., April 15, 1970, p. 17.
2. A. E. Dabiri and R. E. Stickney, Quarterly Progress Report No. 95, Research Laboratory of Electronics, M. I. T., October 15, 1969, p. 19; see especially p. 22, Eq. (1).
3. A. Ellett and V. W. Cohen, Phys. Rev. 52, 509 (1937); J. H. McFee and P. M. Marcus, in Proceedings of Atomic and Molecular Beams Conference (Denver, 1960), p. 178.
4. For a review of literature pertaining to this problem, see L. B. Loeb, Kinetic Theory of Gases (McGraw-Hill Book Co., New York, 2d edition, 1934).
5. W. van Willigen, Phys. Letters 28A, 80 (1968).
6. J. E. Lennard-Jones, Trans. Faraday Soc. 28, 333 (1932).
7. E. H. Kennard, Kinetic Theory of Gases (McGraw-Hill Book Co., New York, 1938), pp. 61-64.
8. P. B. Scott, "Molecular Beam Velocity Distribution Measurements," M. I. T. Fluid Dynamics Research Laboratory Report 65-1, February 1965.
9. W. G. Vincenti and C. H. Kruger, Jr., Physical Gas Dynamics (John Wiley and Sons, Inc., New York, 1965), Chaps. 1 and 2.